Chem. Res. Chin. Univ., 2016, 32(2), 253—260 doi: 10.1007/s40242-016-5404-3

Crystal Structure, Vibrational Studies, Optical Properties and TG-DTA Investigations of a New Chlorocadmate Templated by 1-Methylimidazolium

Melek HAJJI[1] and Taha GUERFEL[1,2*]

1. Laboratory of Electrochemistry, Materials and Environment,

2. Preparatory Institute for Engineering Studies, Kairouan University, 3100 Kairouan, Tunisia

Abstract Chemical preparation, X-ray single crystal diffraction, thermal analysis, electrochemical measurements, IR, Raman and UV spectroscopic investigations of a novel organic-inorganic hybrid material($C_4H_7N_2$)$CdCl_3(H_2O)$(**1**) were described. 1-Methylimidazolium aquapentachlorocadmate(II) crystallized in the monoclinic system with $P2_1/n$ space group. Its structure provided a new interesting example of infinite inorganic layers of $[CdCl_3(H_2O)]_n^{n-}$ centered by (–101) planes. The $[CdCl_5(H_2O)]^-$ anions were interconnected by O—H···Cl hydrogen bonds. Acidic protons of the chloride group were transferred to the organic molecule, giving the singly-protonated cations. The ability of ions to form a spontaneous three-dimensional structure through O—H···Cl and N—H···Cl hydrogen bonds was fully utilized. These hydrogen bonds induced notable vibrational effects. IR and Raman spectra were reported and discussed on the basis of group theoretical analysis and on quantum chemical density theory(DFT) calculation. The molecular HOMO-LUMO compositions and their respective energy gaps were also drawn to explain the activity of our compound. The role of the intermolecular interaction in this crystal was analyzed. The optical study was also investigated by UV-Vis absorption spectrum. Thermal analysis reveals the hydrous character of the compound. Cyclic voltammetry was studied to evaluate the spectral and structural changes accompanying electron transfer.

Keywords Chlorocadmate(II); X-Ray diffraction; Thermal analysis(TG-DTA); Vibrational study; Density functional theory calculation; Cyclic voltammetry

1 Introduction

In recent years, the synthesis and characterization of coordination polymers have been of great interest. This is due to their fascinating structures and potential applications in catalysis, conductivity, porosity, chirality, luminescence, magnetism, spin-transition and non-linear optics[1—8]. The size of the organic cations, their symmetry and ability to form hydrogen bonds determine the physico-chemical properties of these materials[9—11]. Complexes of imidazole derivatives with transition metal ions have attracted much attention thanks to their biological and pharmacological activities, such as antiviral, antimicrobial and antiallergic properties[12—14]. The biological role of the complexes containing an imidazole ring system can be related to the two N atoms, which have different properties. The deprotonated N atom can coordinate to a transition-metal ion, whereas the protonated N atom participates in hydrogen bonding[15—17]. For a better understanding of the principles governing the structural properties of imidazole complexes, especially the role played by hydrogen bonds, we synthesized a new halocadmate templated by 1-methylimidazole. The halocadmate(II) family, in particular the chlorocadmate, is composed of distorted $(CdCl_6)^{2-}$ or $[(CdCl_5(H_2O)]^-$ isolated octahedra or connected corners, edges, or faces forming ribbons, planes or layers[18—20]. The cavities between the inorganic moieties are filled with organic cations in anionic framework through hydrogen bonds and/or electrostatic interactions[21—23]. In this paper, the polymeric complex ($C_4H_7N_2$)$CdCl_3(H_2O)$(**1**) was characterized by X-ray diffraction, TG-DTA measurement, FTIR absorption and FT-Raman scattering. Density functional theory calculation was used in order to perform the structural analysis of the studied molecules. In the light of the theoretical calculation, correlation between FTIR and FT-Raman spectra and computed results help to identify the vibrational modes and provide deeper insights into the bonding and structural features of our compound. With the help of the cyclic voltammetry, some electrochemical measurement was performed.

2 Experimental

2.1 Chemical Preparation

1-Methylimidazolium aquapentachlorocadmate(II) was synthesized according to a previously reported method for similar chlorocadmate[20,24]. Crystals of compound **1** were prepared by slow evaporation, at room temperature, of 300 mL of an aqueous solution of HCl(2.46 mL, 0.03 mol, purity 37%, Aldrich) mixed with $Cd(CO_3)$(1.72 g, 0.01 mol, purity

*Corresponding author. E-mail: taha_guerfel@yahoo.fr

Received October 19, 2015; accepted December 1, 2015.

© Jilin University, The Editorial Department of Chemical Research in Chinese Universities and Springer-Verlag GmbH

98%, Aldrich) and neutralized by 1-methylimidazole(0.821 g, 0.01 mol, purity 99%, Aldrich) with a molar ratio of 3:1:1. During this operation, the solution was vigorously stirred. Scheme 1 gives the main steps of the preparation of compound **1**. When most of the solution was evaporated, elongated transparent colorless prisms were obtained.

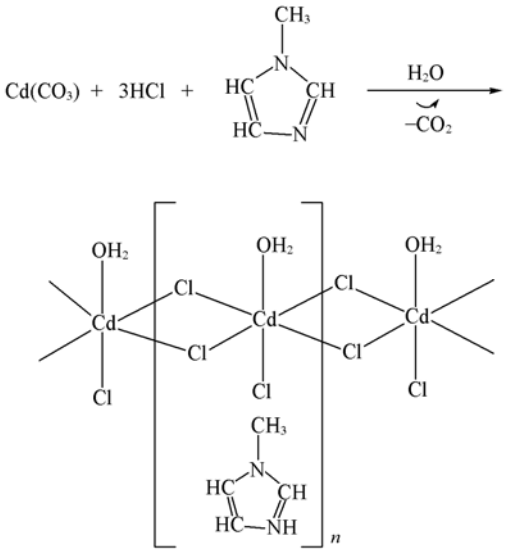

Scheme 1 Synthesis of compound 1

2.2 Single-crystal X-Ray Diffraction

Single crystal X-ray diffraction measurement was carried out at 293 K on a Bruker Enraf-Nonius diffractometer with graphite monochromatized Mo *Kα* radiation in the ω-θ scan mode. Final unit cell dimensions were obtained and refined *via* a set of 25 high-angle reflections. Integration and scaling resulted in the data set, corrected for Lorentz and polarization effects with the aid of XCAD4[25]. The structure of 1-methylimidazolium aquapentachlorocadmate(II) was developed in the centrosymmetric space group $P2_1/n$. The trial structure was obtained by direct methods with resort to SHELXS-97[26], which revealed the position of the cadmium, chlorine, oxygen and most atoms of the organic molecule. The remainder of the structure was found in the subsequent difference Fourier syntheses. There were one $[CdCl_5(H_2O)]^-$ anion and one organic$(C_4H_7N_2)^+$ cation. The final structural refinement was made with F^2 data and the program SHELXL-97[26]. All the hydrogen atoms were located in a difference Fourier map. Anisotropic displacement parameters for all the other atoms were allowed to vary. The anisotropies were found to be moderate. The average density, measured at room temperature with toluene as pycnometric liquid, is in agreement with the calculated density. The cell contains four formula units of the title compound. Crystal data and the results of the final structure refinement are summarized in Table1. Selected bond distances and angles are given in Table 2.

The CCDC reference number is 1050839 for compound **1**.

2.3 Spectroscopic Measurements

Infrared(IR) spectrum was recorded at room temperature

Table 1 Crystal data and structure refinement of compound 1

Compound	$(C_4H_7N_2)CdCl_3(H_2O)$
Crystal system	Monoclinic
Space group	$P2_1/n$
Molar mass	390.78
T/K	293(2)
μ/mm^{-1}	0.2949
Wavelength of radiation used/nm	0.07107
a/nm	1.1454(6)
b/nm	0.7476(4)
c/nm	1.1768(6)
β/(°)	98.997(7)
V/nm^3	0.9952(9)
Z	4
Crystal size	0.38 mm×0.31 mm×0.25 mm
F(000)	752
θ range	2.31°—26.97°
hkl range	$-14\leqslant h\leqslant 14$, $-2\leqslant k\leqslant 9$, $0<l<14$
Reflection collected	2961
Independent reflection, R_{int}	2166(0.0059)
Maximum and minimum transmission	0.5417/0.3355
Restraint/independent parameter	2/130
GOF	1.04
Final R indices[$I>2\sigma(I)$]	$R_1{}^a$=0.0329, $wR_2{}^b$=0.0873
$\Delta\rho_{min}$ and $\Delta\rho_{max}$/(e·nm^{-3})	−852/607

a. $R_1=\sum\|F_0|-|F_c\|/\sum|F_0|$; *b*. $wR_2=\{\sum w(F_0^2-F_c^2)^2/\sum w(F_0^2)^2\}^{1/2}$.

Table 2 Selected bond lengths(nm) and bond angles(°) for compound 1*

Species	Bond	Bond length/nm		Bond angle/(°)	
		Exp.	Calcd.	Exp.	Calcd.
Organic cation	N1—C1	0.1483(8)	0.1484		
	N1—C2	0.1311(8)	0.1351		
	N1—C4	0.1372(7)	0.1412		
	N2—C2	0.1311(8)	0.1341		
	N2—C3	0.1342(8)	0.1403		
	C3—C4	0.1326(9)	0.1341		
	C1—N1—C2			125.7(5)	125.4
	C1—N1—C4			125.5(5)	126.1
	C2—N1—C4			108.8(5)	108.5
	C2—N2—C3			109.9(6)	109.4
	N1—C2—N2			107.5(5)	107.6
	N2—C3—C4			107.3(5)	107.1
	N1—C4—C3			106.5(5)	107.3
$CdCl_5(H_2O)$ octahedron	Cd—O_W	0.2401(4)	0.2284		
	Cd—Cl1	0.2566(1)	0.2490		
	Cd—Cl2	0.2634(1)	0.2295		
	Cd—Cl3	0.2598(1)	0.2258		
	Cd—Cl2#1	0.2650(1)	0.2364		
	Cd—Cl3#2	0.2596(1)	0.2260		
	Cl1—Cd—Cl2			96.0(4)	101.1
	Cl1—Cd—Cl3			95.3(4)	94.1
	Cl1—Cd—Cl2#1			93.7(4)	95.0
	Cl1—Cd—Cl3#2			94.7(4)	91.3
	Cl2—Cd—O_W			86.5(1)	83.1
	Cl2—Cd—Cl3			91.4(3)	89.5
	Cl2—Cd—Cl3#2			87.5(3)	88.5
	Cl3—Cd—O_W			85.6(1)	85.3
	Cl3—Cd—Cl2#1			87.1(3)	89.5
	Cl2#1—Cd—O_W			83.8(1)	80.9
	Cl2#1—Cd—Cl3#2			92.4(3)	91.0
	Cl3#2–Cd–O_W			84.4(1)	85.4

* Symmetric codes: #1: $-x+1/2$, $y-1/2$, $-z+1/2$; #2: $-x+1/2$, $y+1/2$, $-z+1/2$.

on a Biored FTS 6000 FTIR spectrophotometer in a region of 400—4000 cm^{-1}. Thin transparent pellet was made by compacting an intimate mixture obtained by shaking 2 mg of the sample in 100 mg of KBr.

Raman spectrum was recorded on a Jobin Yvon Horiba HR800 LabRAM spectrometer in a range of 200—2000 cm^{-1}.

UV-Vis spectrum was measured on a high-resolution Beckman DU640 spectrophotometer in a range of 200—800 nm in aqueous solution.

2.4 Computational Details

The molecular structure of our compound was fully optimized without any constraint by virtue of the DFT approach and effective core potentials(ECPs) in order to represent the metal(LANL2DZ basis and ECP built-in). The B3LYP method with 6-31+G(d,p) basis set was used for all the atoms except for cadmium[27,28]. The calculated optimized structure was used in the vibrational frequency calculations[29—31]. The molecular geometry was not limited, and all the calculations(vibrational wavenumbers, optimized geometric parameters and other molecular properties) were performed *via* Gauss View molecular visualization program[32] and Gaussian 09W program package[33]. Furthermore, the calculated vibrational frequencies were clarified by means of the potential energy distribution (PED) analysis of all the fundamental vibration modes by using VEDA 4 program[34].

2.5 Thermal Behavior

Setaram TG-DTA 92 thermoanalyser was used to perform a thermal treatment on compound **1**. TG-DTA thermograms were obtained with a sample of 40.23 mg in an open platinium crucible heated in air at 5 °C/min from room temperature to 500 °C. An empty crucible was used as reference.

2.6 Cyclic Voltammetry Analyses

Electrochemical measurement was performed in a conventional electrochemical cell containing a three-electrode system ensuring stable positioning of the electrodes and an agitation of the solution. The glassy carbon electrode was the working electrode, a platinum electrode was used as auxiliary electrode and a saturated calomel electrode served as a reference electrode.

3 Results and Discussion

3.1 Structure Description

The atomic arrangement of 1-methylimidazolium aquapentachlorocadmate(II) is described by a typical thick layered organization containing all its components centered by (–101) planes(Fig.1). Each $[CdCl_5(H_2O)]^-$ groupment is surrounded by two organic molecules and two $[CdCl_5(H_2O)]^-$ anions, issuing two N—H···Cl and two O—H···Cl hydrogen bonds. Interatomic distances and bond angles describing $[CdCl_5(H_2O)]^-$ anions are reported in Table 2. The Cd—X distances(X=Cl or OH_2) vary from 0.2401(4) nm to 0.2650(1) nm with an average value $\langle d(Cd—X)\rangle$ being 0.2574 nm. The Cl—X distances vary from 0.3358(4) nm to 0.3865(2) nm with an average value $\langle d(Cl—X)\rangle$ being 0.3628 nm. The Cl—Cd—X angles(with Cl and X in *cis*-positions) vary from 83.8(1)° to 96.0(4)° with an average value of 89.87°. The calculation of distortion indices of angles and distances in $[CdCl_5(H_2O)]^-$ anions according to the method of Baur[35] shows a more pronounced distortion of Cl—X distances and Cl—Cd—X angles when compared to Cd—X distances. The slight differences between Cd—X distances are due to the different environments of chlorine atoms. The length of Cd—Cl distances depends on the number and strength of hydrogen bonds in which the chlorine atom is engaged. This was noted in other structures containing Cl^- anion associated with several metals[24]. The projection of atomic arrangement along the $[\bar{1}01]$ crystallographic direction(Fig.2) shows $[CdCl_5(H_2O)]^-$ octahedra sharing an edge Cl—Cl to form the chains of formula: $[CdCl_3(H_2O)]_n^{n-}$ parallel to b axis. Interconnection between different chains *via* hydrogen bonds according to [101] direction is insured by water molecules to form anionic layers. The protonation of the asymmetric molecule 1-methylimidazole according to the experimental protocol led to 1-methylimidazolium cation with the protonation of one nitrogen atom. The carbon and nitrogen atoms of this cation are Planar(mean deviation=0.0043) that are localized on general positions. The organic molecule of the asymmetric unit possesses no internal symmetry. The interatomic distances and

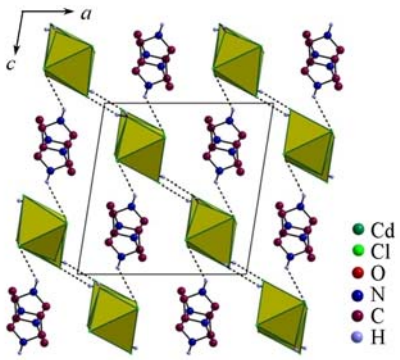

Fig.1 Projection along the *b* axis of the atomic arrangement

The H atoms were omitted for clarity; H-bonds were represented by dashed lines.

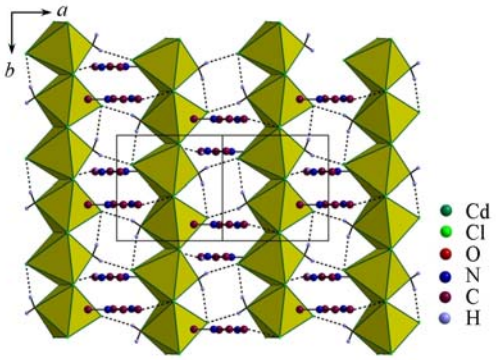

Fig.2 Projection along the $[\bar{1}01]$ direction of the atomic arrangement

angles describing this cation are similar to intramolecular bond distances and angles usually reported for such species[36—38]. The C—N distances vary between 0.1311(8) and 0.1483(8) nm with an average value $\langle d(\mathrm{C—N})\rangle$ of 0.1364 nm. The angles vary between 106.5(5)° and 125.7(5)° with an average value of 113.0°. From experimental(X-ray) and calculated geometric parameters of $(C_4H_7N_2)CdCl_3(H_2O)$ shown in Table 2, it is illustrated that some of the calculated bond lengths and bond angles are found to be slightly different from the experimental ones. These discrepancies may be due to the presence of intermolecular hydrogen bonding. It can also be explained by the fact that the calculations relate to the isolated molecule where the intermolecular Coulombic interactions with the neighboring molecules are absent, whereas the experimental result corresponds to interacting molecules in the crystal lattice. The protonated nitrogen atom of the organic cation shares hydrogen bonds, of N—H···Cl type, with $[CdCl_5(H_2O)]^-$ chlorine atoms. The structural arrangement contains two types of hydrogen bonds: N—H···Cl and O—H···Cl. The water molecule plays a very important role in the cohesion of the bi-dimensional arrangement. It contributes with its two hydrogen atoms to the binding of two $[CdCl_5(H_2O)]^-$ anions. The geometrical parameters of these bonds are reported in Table 3. The crystalline structure does not contain the same number of donors and acceptors involved in the hydrogen bonding system: one N(H) and two O(H) as donors and two chlorine atoms(Cl2 and Cl1) as acceptors. The cohesion and stability of the crystalline building are maintained by the two-dimensional network of hydrogen bonds and van der Waals interactions between successive layers.

Table 3 Bond lengths and angles in the hydrogen-bonding scheme*

D—H···A	*d*[N(O)—H]/ nm	*d*(H···Cl)/ nm	*d*[N(O)···Cl]/ nm	∠N(O)—H···Cl/ (°)
N2—H(N2)···Cl2#1	0.079(7)	0.276(7)	0.3309(6)	128(7)
OW—H(1W)···Cl1#2	0.079(2)	0.243(4)	0.3206(4)	164(4)
OW—H(2W)···Cl1#3	0.080(2)	0.245(4)	0.3206(4)	158(4)

* Symmetric codes: #1: $-x+1/2$, $y-1/2$, $-z+1/2$; #2: $-x+1/2$, $y+1/2$, $-z+1/2$; #3: $x+1/2$, $-y+1/2$, $z+1/2$.

3.2 Vibrational Study

In order to give more information about the crystal structure, we studied the vibrational properties of compound **1** using Raman scattering and infrared absorption. Taking into account the effect of intermolecular interactions on geometrical parameters, we considered the $[CdCl_5(H_2O)]^-$ anion and one organic cation linked *via* N—H···Cl hydrogen bond. All the parameters were allowed to relax and all the calculations converged to an optimized geometry which corresponds to an energy minimum as revealed by the lack of imaginary values in the calculated wavenumbers. The vibrational modes were conducted by the visual inspection of modes animated by using GaussView program[32] and by comparison with the experimental results reported in the literature for similar compounds. The computed wavenumbers corresponding to different modes along with detailed assignments are listed in Table S1(see the Electronic Supplementary Material of this paper). For visual comparison, the observed and simulated Raman and IR spectra are presented, respectively, in Fig.3 and Fig.4. The computed fundamental vibrational frequencies are slightly different from the corresponding experimental values. These discrepancies are explained by the combination of electron correlation effects and by the fact that experimental value contains the anharmonic oscillation frequency while the calculated value is a harmonic frequency. These discrepancies may be also due to the intermolecular hydrogen bonding effects.

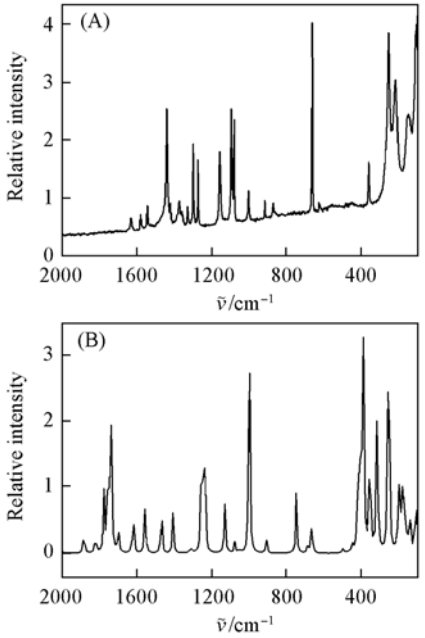

Fig.3 Observed(A) and calculated(B) FT-Raman spectra of compound 1

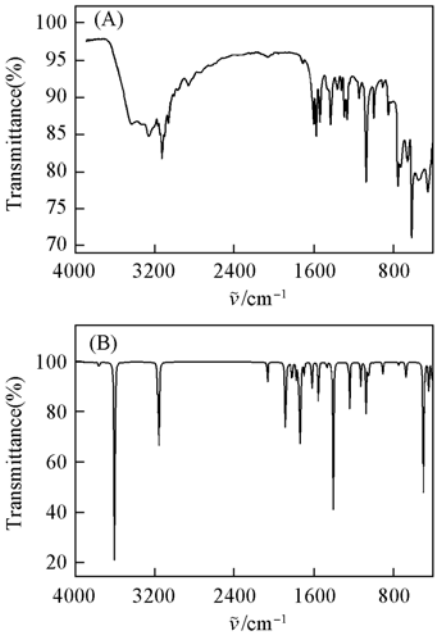

Fig.4 Observed(A) and calculated(B) FTIR spectra of compound 1

The splitting of F_{1u} stretching mode of $CdCl_5(H_2O)$ into three components at 386, 371 and 361 cm^{-1} in the Raman spectrum depicted in Fig.3 corroborates the symmetry lowering

of $CdCl_5(H_2O)$ in the solid state toward the C_1 symmetry[39]. The symmetric stretching modes $\nu_1(A_{1g})$ and $\nu_2(E_g)$ are found, respectively, as one peak at 256 cm^{-1} and two peaks at 223 and 218 cm^{-1}. The bending modes are observed at lower frequencies. The hydrogen atoms of water molecules act as proton-donors in hydrogen bonds of O_W—H···Cl type. $H2_W$ atom participates in a very weak hydrogen bond in which Cl1 chlorine atom acts as a proton acceptor. According to X-ray data, the length of this bond is 0.2452 nm. The second hydrogen atom of water molecule, $H1_W$ atom is engaged in a stronger hydrogen bond in which Cl1 chlorine atom acts as a proton acceptor. For this hydrogen bond interaction, the length resulted from structural investigations equals 0.2434 nm. Owing to such a difference in the lengths of the above mentioned bonds, the vibrations of water molecules manifest themselves as two independent O—H stretching vibrations giving medium infrared bands at 3441 and 3337 cm^{-1}. Their Raman counterparts may not be visible in the spectra, due to the insufficient sensitivity of Raman detector above 3200 cm^{-1}. The presence of water molecules is clearly manifested by the strong band observed in Raman spectrum at 1545 cm^{-1}. This band was attributed to in-plane deformation type of vibrations of water molecules $\delta(H_2O)$[40]. The corresponding band due to the out-of-plane bending type of vibration of water molecule $\gamma(H_2O)$ is observed in IR spectrum at 662 cm^{-1} and at 618 cm^{-1} in Raman spectrum.

Numerous functional and skeletal groups, such as CH_3, CH, NH, N—C, N═C, C═C, CNC, NCC and NCN are present in 1-methylimidazolium cation. These groups are manifested in IR and Raman spectra in different ranges with different intensities. For the assignments of CH_3 group, one can expect that 9 fundamentals can be associated with each CH_3 group, namely, the symmetrical stretching(CH_3 symmetric stretch) and asymmetrical stretching(CH_3 asymmetric stretch), in-plane stretching modes(*i. e.*, in-plane hydrogen stretching modes) and the symmetrical(CH_3 symmetric deform) and asymmetrical(CH_3 asymmetric deform) deformation modes; in-plane rocking(CH_3 ipr), out-of-plane rocking(CH_3 opr), and twisting(tCH_3) bending modes. For the methyl group compounds, the asymmetric stretching mode appeared in a range of 2965—3005 cm^{-1}, and the symmetric stretching mode appeared in a range of 2815—2860 cm^{-1}[41]. The IR band at 2967 cm^{-1} is asymmetric stretching. The symmetric methyl stretching band appeared at 2820 and 2859 cm^{-1}. The asymmetric deformation mode appeared in a range of 1445—1485 cm^{-1} and symmetric deformation mode appeared in a range of 1420—1460 cm^{-1}[41]. The IR bands at 1535 and 1484 cm^{-1} are considered as asymmetric deformation vibrations. The IR band at 1330 cm^{-1} is a symmetric deformation mode. The CH_3 deformation absorption occurs at 1436 cm^{-1}. This vibration is known as umbrella mode that overlaps with CN ring stretching vibrations for the title compound. The C—H stretching vibration occurs above 3000 cm^{-1} and is typically exhibited as a multiplicity of weak to moderate bands, compared with the aliphatic C—H stretch[42]. In our present work, the C—H stretching vibration of imidazolium ring was observed at 3103 cm^{-1} in FTIR spectrum. The same vibration was calculated at 3164 cm^{-1} and it showed a good correlation with the experimental data. The in-plane C—H bending vibrations appeared in a range of 1300—1000 cm^{-1} and the out-of-plane bending vibrations occured in a frequency range of 1000—750 cm^{-1}[43]. The C—H in-plane bending vibrations of imidazolium were coupled with ring C═C and C—N stretching modes as is evident from PED. IR active C—H in-plane bending vibration of the title molecule appeared at 1272 cm^{-1} with a PED contribution of 24%. The Raman active bands at 1299, 1273 and 1158 cm^{-1} correspond to the C—H in-plane bending modes. The theoretically predicted wavenumbers at 1259, 1248 and 1217 cm^{-1} by DFT method are attributed to the C—H in-plane bending vibrations and are in line with the measured wavenumbers. The C—H out-of-plane bending vibrations were observed at 915 and 854 cm^{-1} in FTIR and at 917 and 871 cm^{-1} in FT-Raman and the corresponding vibrations were calculated at 937 and 859 cm^{-1}. The vibrations belonging to N—H stretching always occur in a region of 3450—3250 cm^{-1} which, being the characteristic region, allows for ready identification of this structural feature[43—46]. In this region, the bands are not affected appreciably by the nature of the substituents. In this study, the FTIR band observed at 3259 cm^{-1} is assigned to N2—H(N2) stretching vibration. The theoretically-calculated values at 3420 cm^{-1} are assigned to the N—H stretching vibration. The PED of this mode is 93%, thus suggesting that this is an almost pure mode. Most of the computed frequencies are assigned to C═C stretching vibrations, and thus almost coincide with experimental data without scaling. The C═C stretching modes of the imidazolium group are expected in a range from 1650 cm^{-1} to 1200 cm^{-1}. The actual position of these modes is determined not so much by the nature of the substituents but by the form of the substitution around the ring[47]. The bands at 1623, 1608, 1597, and 1272 cm^{-1} in FTIR and the bands at 1631, 1590, 1578, and 1299 cm^{-1} in FT-Raman were observed due to the C═C stretching vibrations. The theoretical wavenumbers for C═C stretching vibrations were predicted at 1641, 1592, 1563 and 1259 cm^{-1} and coincided very well with the experimental data as well as with the literature data. The identification of C═N and C—N vibrations is a very difficult task, since the mixing of several bands is possible in this region. In the case of 1-methylimidazolium, the C—N stretching bands are found to be at 1300 and 1272 cm^{-1}. Hachula *et al*.[36] identified the stretching frequency of the C═N band in imidazole at 1438 cm^{-1}. In our present work, for 1-methylimidazolium molecule, the band observed at 1465, 1378 cm^{-1} in FTIR spectrum and at 1440, 1373 cm^{-1} in FT-Raman spectrum were assigned to C═N stretching vibrations. The theoretically-computed value of C═N stretching vibration also falls in a region of 1451—1354 cm^{-1}. The CNC in-plane bending vibrations are observed at 1001, 732, and 552 cm^{-1} in FTIR and at 1002, 663, and 457 cm^{-1} in FT-Raman. These assignments are in good agreement with the values in the literature[48,49]. The CCN in-plane and out-of-plane bending vibrations were also predicted at 1076 and 934 cm^{-1}, respectively and exactly correlated with the measured FTIR wavenumbers.

It is well known that hydrogen bonding brings about remarkable wavenumber shifts. While the intermolecular

hydrogen bonds give rise to broad bands, intramolecular hydrogen bonds will produce sharp and well resolved bands. X-Ray diffraction analysis of the compound revealed that the structure was described by a typically thick-layered organization containing all its components. Each $[CdCl_5(H_2O)]^-$ groupment is surrounded by two organic molecules and two anions, issuing two N—H···Cl and two O—H···Cl hydrogen bonds. The hydrogen bond lengths of N(O)—H···Cl types range from 0.2434 nm to 0.2758 nm. The assignment of the stretching ν[O(N)—H···Cl], the in-plane bending δ[O(N)—H···Cl] and the out-of-plane bending γ[O(N)—H···Cl] vibrations to the respective bands was made on the basis of our calculations as a preliminary source and also on the basis of classical hydrogen bond theory presented in several reference works[50,51]. The three broad bands in IR spectrum located at 3441, 3337 and 3259 cm^{-1} are accredited to ν[O(N)—H···Cl] mode, whereas the DFT calculated ones to their positions are at 3597, 3483 and 3420 cm^{-1}. The wavenumbers of this mode were shifted towards lower values. As seen in ν[O(N)—H···Cl] stretching, wavenumbers were clearly lower than the calculated values and the bending wavenumbers were not much different from the expected range, which indicates that the linear distortion is much greater than the angular distortion.

3.3 Frontier Molecular Orbital Analysis

The frontier molecular orbitals termed highest occupied molecular orbital(HOMO) and lowest unoccupied molecular orbital(LUMO) play an important role in the electric and optical properties, as well as in UV-Vis spectra and chemical reactions[52]. These orbitals determine the way that the molecule interacts with other species. The LUMO as an electron acceptor represents the ability to obtain an electron, but HOMO represents the ability to donate the electron. The energy gap between HOMO and LUMO is a critical parameter in determining the electrical transport properties of molecules[53]. Recently, the energy gap has been used to prove the bioactivity from intermolecular charge transfer[54,55]. A molecule with a small frontier orbital gap is more polarizable and is generally associated with a high chemical reactivity and a low kinetic stability. It is also termed as soft molecule[56]. The contour surfaces of the frontier molecular orbitals are sketched in Fig.5. The HOMO is localized on the $[CdCl_5(H_2O)]^-$ parts and LUMO is distributed on the $[CdCl_5(H_2O)]^-$ groups without water molecules. The LUMO energy is –5.464 eV and the HOMO energy is –9.433 eV. The HOMO-LUMO gap($\Delta E = E_{LUMO} - E_{HOMO}$) of compound **1** is found to be 3.696 eV. The title compound is dynamically more stable due to the large energy gap.

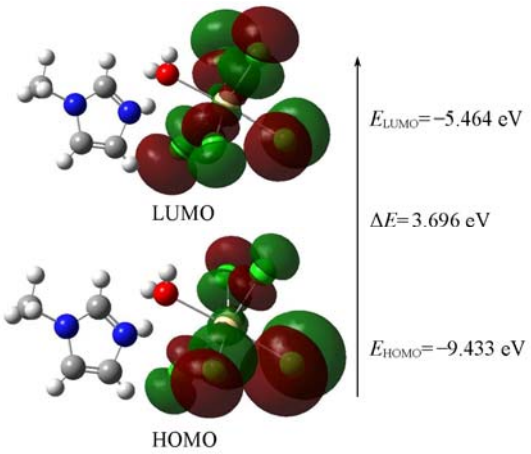

Fig.5 Frontier molecular orbitals of compound 1

3.4 UV-Visible Absorption Spectroscopy

The electronic spectrum shown in Fig.6 reveals an absorption band centered at 314 nm(3.96 eV, 31948 cm^{-1}, ε_{max}=9120 $mol^{-1}\cdot cm^{-1}$), which is due to the band gap absorption and it is assigned to the excitation of free electron-hole pairs within the $[CdCl_5(H_2O)]^-$. This peak is mainly due to the absorption between Cl(3*p*) and Cd(5*s*)(band to band) which suggests that the material behaves as a semiconductor[57].

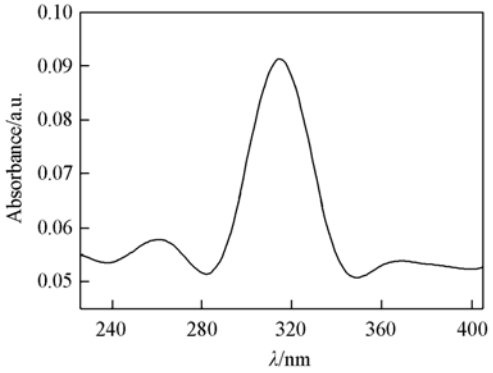

Fig.6 UV-Vis spectrum of compound 1

3.5 Thermal Behavior

From the TGA mass loss curve(Fig.7), we deduced that there is one water molecule per formula unit $(C_4H_7N_2)CdCl_3(H_2O)$(calculated mass loss 5.63%, observed mass loss 5.43%). The removal of water molecule, observed in a temperature range of 75—128 °C, is related to the first endothermic peak on the DTA curve with maximum elimination at 95 °C. The weakness of the hydrogen bonds in the network explained the departure of the water molecule in this low temperature range. The second and third endothermic peaks, observed respectively at 142 and 160 °C, can be attributed to weak phase transitions. However, the stability of the compound is not very high, since it melts at 228 °C and decomposes in a

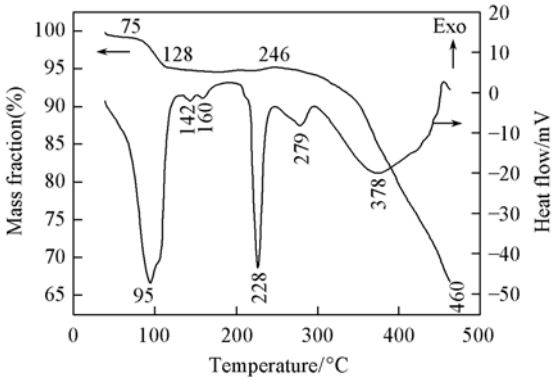

Fig.7 TG-DTA curves of compound 1

range of 246—500 °C with a maximum elimination at 378 °C. Within this temperature range, a rather bad smell escaped from the resulting melting black compound.

3.6 Electrochemical Measurements

In order to discuss the redox properties of our compound, the cyclic voltammogram was performed in a 10^{-3} mol/L sample solution in acetonitrile(CH_3CN), containing tetrabutylammonium tetrafluoroborate(TBAF) as supporting electrolyte. The range of potential studied was in between 0 and –2.25 V at a scan rate of 100 mV/s. Two successive reduction waves in the negative potential region were observed, demonstrating that electroactive species can have two different oxidation states(Fig.8). Therefore, observed waves can be respectively assigned to Cd(II)/Cd(I)(E_{pc}= –1.30 V, I_{pc}= –3.77× 10^{-5} A) and Cd(I)/Cd(0)(E_{pc} = –1.65 V, I_{pc} = –4.96×10^{-5} A) couple processes[58—60]. In addition to these waves, there is one oxidation wave at –1.35 V appeared upon measuring in the opposite direction. Thus, it does not correspond to Cd(0)/Cd(II) process. The peak separation between anodic and catodic peak potentials(E) was the highest at a scan rate of 100 mV/s. The large potential difference separation(E) at the glassy-carbon electrode is an indicative of an electrochemically irreversible process.

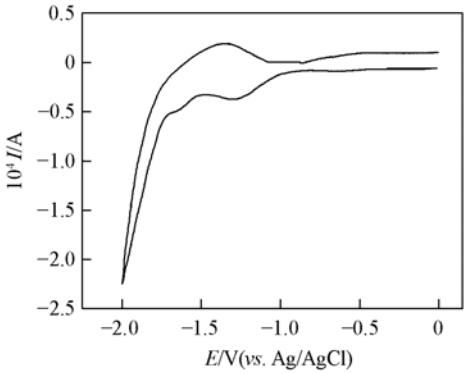

Fig.8 Cyclic voltammogram of compound 1

4 Conclusions

Crystal structure, X-ray diffraction study, optical properties, thermal behavior and vibrational and PED analysis using the density functional density(DFT) approach of $(C_4H_7N_2)CdCl_3(H_2O)$ have been investigated and reported. We studied the molecular parameters and frequency assignments of the compound using the FTIR and FT-Raman spectra. The good agreement of the calculated and observed vibrational spectra revealed the advantages of a smaller basis set for quantum chemical calculations. HOMO-LUMO analysis of the title compound explains the eventual charge transfer interactions taking place within the molecule. Electrochemical measurement by cyclic voltammetry was performed, proving the cadmium oxidation state. Our overall simulated results for different molecular properties of our compound were obtained for the first time. We hope that they will be helpful in the synthesis, design and application of new organometallic chlorides based on cadmium.

Supplementary Material

CCDC No. 1050839 contains the supplementary crystallographic data for this article. These data can be obtained free of charge via www.ccdc.cam.ac.uk/data_request/cif, by emailing data_request@ccdc.cam.ac.uk, or by contacting The Cambridge Crystallographic Data Center, 12 Union Road, Cambridge CB2 1EZ, UK. Fax: C44 1223336033.

Electronic Supplementary Material

Supplementary material is available in the online version of this article at http://dx.doi.org/10.1007/s40242-016-5404-3.

References

[1] Ma S., Zhou H. C., *Chem. Commun.*, **2010**, *46*, 44
[2] Murray L. J., Dinca M., Long J. R., *Chem. Soc. Rev.*, **2009**, *38*, 1294
[3] Kuppler R. J., Timmons D. J., Fang Q. R., Li J. R., Makal T. A., Young M. D., Yuan D., Zhao D., Zhuang W., Zhou H. C., *Coord. Chem. Rev.*, **2009**, *253*, 3042
[4] Wang J., Luo X., Yuan Y., Zhang L., *Chem. Res. Chinese Universities*, **2015**, *31*(4), 503
[5] Takaishi S., Hosoda M., Kajiwara T., Miyasaka H., Yamashita M., Nakanishi Y., Kitagawa Y., Yamaguchi K., Kobayashi A., Kitagawa H., *Inorg. Chem.*, **2008**, *48*, 9048
[6] Kitagawa S., Kitaura R., *Angew. Chem., Int. Ed. Eng.*, **2004**, *43*, 2334
[7] Smida M., Litaiem H., Dammak M., Garcia-Granda S., *Chem. Res. Chinese Universities*, **2015**, *31*(1), 16
[8] Kahn O., *Acc. Chem. Res.*, **2000**, *33*, 647
[9] Ma T. H., Yu J. H., Ye L., Xu J. Q., Wang T. G., Lu C. H., *J. Mol. Struct.*, **2003**, *47*, 654
[10] Lü L., Mu B., Li N., Huang R., *Chem. Res. Chinese Universities*, **2015**, *31*(5), 712
[11] Perpétuo G. J., Janczak J., *J. Mol. Struct.*, **2013**, *1041*, 127
[12] Cheng J., Xie J., Lou X., *Bioorg. Med. Chem. Lett.*, **2005**, *15*, 267
[13] Sheng J., Nguyen P. T. M., Baldeck J. D., Olsson J., Marquis R. E., *Arch. Oral Bio.*, **2006**, *51*, 1015
[14] Nakano H., Inoue T., Kawasaki N., Miyataka H., Matsumoto H., Taguchi T., Inagaki N., Nagai H., Satoh T., *Bioorg. Med. Chem.*, **2000**, *8*, 373
[15] Huang X. C., Zhang J. P., Lin Y. Y., Yu X. L., Chen X. M., *Chem. Commun.*, **2004**, (9), 1100
[16] Abuskhuna S., McCann M., Briody J., Devereux M., McKee V., *Polyhedron*, **2004**, *23*, 1731
[17] Gong Y., Hu C., Li H., Pan W., Niu X., Pu Z., *J. Mol. Struct.*, **2005**, *740*, 153
[18] Bourdeau C. L., Chanh N. B., Duplessix R., Gallois B., *J. Phys. Chem. Solids*, **1993**, *349*, 54
[19] Puget R., Jannin M., de Brauer C., Perret R., *Acta Cryst.*, **1991**, *C47*, 1803
[20] Amamou W., Feki H., Chniba-Boudjada N., Zouari F., *J. Mol. Struct.*, **2014**, *169*, 1059
[21] Xu R., *Acta Cryst.*, **2009**, *E65*, m951
[22] Glaoui M., Zeller M., Jeanneau E., BenNasra C., *Acta Cryst.*, **2010**, *E66*, m895
[23] Xu M., Liu Z., Fan R., Gao S., Chen S., Yang Y., *Chem. Res. Chinese Universities*, **2014**, *30*(5), 720
[24] Hajji M., Gharbi A., Guerfel T., *J. Inorg. Organomet. Polym.*, **2014**, *24*, 766

[25] Harms K., Wocadlo S., *XCAD4*, University of Marburg, Marburg, **1995**

[26] Sheldrick G. M., *Acta Cryst.*, **2008**, *A64*, 112

[27] Lindsay E. R., Jeffrey H. P., Richard L. M., *J. Chem. Theory Comput.*, **2008**, *4*(7), 1029

[28] Liu C., Zhang D., Gao M., Liu S., *Chem. Res. Chinese Universities*, **2015**, *31*(4), 597

[29] James W. H., Buchanan E. G., Müller C. W., Dean J. C., Kosenkov D., Slipchenko L. V., Guo L., Reidenbach A. G., Gellman S. H., Zwier T. S., *J. Phys. Chem.*, **2011**, *A115*, 13783

[30] Young D. C., *Computational Chemistry*: *A Practical Guide for Applying Techniques to Real-World Problems(Electronics)*, John Wiley and Sons, Academic Press, New York, **2001**

[31] Sert Y., Al-Turkistani A. A., Al-Deeb O. A., El-Emam A. A., Ucun F., Çırak Ç., *Spectrochim. Acta A*, **2014**, *120*, 97

[32] Frish A., Nielsen A. B., Holder A. J., *Gauss View User Manual*, Gaussian Inc., Pittsburg, PA, **2001**

[33] Frisch M. J., Trucks G. W., Schlegel H. B., Scuseria G. E., Robb M. A., Cheeseman J. R., Scalmani G., Barone V., Mennucci B., Petersson G. A., Nakatsuji H., Caricato M., Li X., Hratchian H. P., Izmaylov A. F., Bloino J., Zheng G., Sonnenberg J. L., Hada M., Ehara M., Toyota K., Fukuda R., Hasegawa J., Ishida M., Nakajima T., Honda Y., Kitao O., Nakai H., Vreven T., Montgomery J. A. Jr., Peralta J. E., Ogliaro F., Bearpark M., Heyd J. J., Brothers E., Kudin K. N., Staroverov V. N., Kobayashi R., Normand J., Raghavachari K., Rendell A., Burant J. C., Iyengar S. S., Tomasi J., Cossi M., Rega N., Millam J. M., Klene M., Knox J. E., Cross J. B., Bakken V., Adamo C., Jaramillo J., Gomperts R., Stratmann R. E., Yazyev O., Austin A. J., Cammi R., Pomelli C., Ochterski J. W., Martin R. L., Morokuma K., Zakrzewski V. G., Voth G. A., Salvador P., Dannenberg J. J., Dapprich S., Daniels A. D., Farkas Ö., Foresman J. B., Ortiz J. V., Cioslowski J., Fox D. J., *Gaussian 09*, *Revision A.1*, Gaussian Inc., Wallingford CT, **2009**

[34] Jamròz M. H., *Spectrochim. Acta Part A*, **2013**, *114*, 220

[35] Baur W. H., *Acta Cryst*., **1974**, *B13*, 1195

[36] Hachula B., Pedras M., Nowak M., Kusz J., Pentak D., Borek J., *J. Serb. Chem. Soc*., **2011**, *76*(2), 235

[37] Therrien B., Beauchamp A. L., *Acta Cryst*., **1993**, *C49*, 1303

[38] Zhang S., Wang S., Wen Y., Jiao K., *Molecules*, **2003**, *8*, 866

[39] Nakamoto K., *Infrared and Raman Spectra of Inorganic and Coordination Compounds*, *Part A: Theory and Applications in Inorganic Chemistry*, *6th Ed*., Wiley, Hoboken, **2009**

[40] Haile S. M., Calkins P. M., Boysen D., *J. Solid State Chem.*, **1998**, *139*, 373

[41] Socrates G., *Infrared Characteristic Group Frequencies*, Wiley, New York, **1980**

[42] Coates J., Meyers R. A., *Interpretation of Infrared Spectra: A Practical Approach*, John Wiley and Sons Ltd., Chichester, **2000**

[43] Silverstein M., Clayton Basseler G., Morill C., *Spectrometric Identification of Organic Compounds*, Wiley, New York, **1981**

[44] Karabacak M., Ahin E. S, Çınar M., Erol I., Kurt M., *J. Mol. Struct.*, **2008**, *886*, 148

[45] Zavadov I. A., Maklakov L. I., Atomvmyan E. G., *Russ. Chem. Bull.*, **1998**, *47*, 293

[46] Furer V. L., *J. Appl. Spectrosc.*, **1990**, *53*, 860

[47] Bellamy L. J., *The Infrared Spectra of Complex Molecules*, *3rd Ed*., Wiley, New York, **1975**

[48] Peesole R. L., Shield L. D., McWillam I. C., *Modern Methods of Chemical Analysis*, Wiley, New York, **1976**

[49] Socrates G., *IR and Raman Characteristics Group Frequencies Tables and Charts*, *3rd Ed*., Wiley, Chichester, **2001**

[50] Schuster P., Zundel G., Sandorfy C., *The Hydrogen Bond Recent Developments in Theory and Experiments*, North-Holland Publishing Company, Amsterdam, New York, Oxford, **1976**

[51] Geffrey G. A., *An Introduction to Hydrogen Bonding*, Academic Press, Oxford, **1977**

[52] Fleming I., *Frontier Orbitals* and *Organic Chemical Reactions*, John Wiley and Sons, New York, **1976**

[53] Fukui K., *Science*, **1982**, *218*, 747

[54] Padmaja L., Ravikumar C., Sajan D., Joe I. H., Jayakumar V. S., Pettit G. R., Nielsen O. F., *J. Raman Spectrosc.*, **2009**, *40*, 419

[55] Ravikumar C., Joe I. H., Jayakumar V. S., *Chem. Phys. Lett.*, **2008**, *460*, 552

[56] Fleming I., *Frontier Orbitals and Organic Chemical Reactions*, Wiley and Sons, New York, **1976**

[57] Lee S. K., Choi H. S., *Bull. Korean Chem. Soc.*, **2001**, *22*, 463

[58] Deveci P., Taner B., Kllç Z., Solak A. O., Arslan U., Özcan E., *Polyhedron*, **2011**, *30*, 1726

[59] Torres E. L., Mendiola M. A., *Polyhedron*, **2005**, *24*, 1435

[60] Feng X., Li Z. F., Xue S. F., Tao Z., Zhu Q. J., Zhang Y. Q., Liu J. X., *Inorg. Chem.*, **2010**, *49*, 7638